Site-Specific Evolution of Surface Stress during the Room-Temperature Oxidation of the Si(111)-(7 × 7) Surface

N. T. Kinahan, D. E. Meehan, T. Narushima,* S. Sachert,† and J. J. Boland‡

School of Chemistry and Centre for Research on Adaptive Nanostructures and Nanodevices (CRANN), Trinity College Dublin, Dublin 2, Ireland

K. Miki

Organic Nanomaterials Center (ONC), National Institute for Materials Science (NIMS), Tsukuba, Ibaraki 305-0044, Japan

(Received 18 December 2009; published 5 April 2010)

The reaction of molecular oxygen with the Si(111)-7 × 7 surface is investigated at room temperature using *in situ* scanning tunneling microscopy and surface stress measurements to reveal the quantitative relationship between site-specific oxygen coverage and a decrease in tensile surface stress. This relationship is described using a modified form of the reaction model originally proposed by Dujardin *et al.* We show that the decrease in tensile surface stress is greatest for the faulted subunits of the 7 × 7 cell and determine the stress signatures of different reaction products, including the absence of long-lived metastable species with a unique stress signature.

DOI: 10.1103/PhysRevLett.104.146101 PACS numbers: 68.43.−h, 68.37.Ef, 68.47.Fg, 82.65.+r

The oxidation of silicon is one of the most important and widely studied reactions. In spite of this, controversy still surrounds the details of the room-temperature reaction mechanism, particularly with regard to the Si(111)-7 × 7 surface [1–10]. A widely accepted model proposed by Dujardin *et al.* [11] revealed that oxidation is a consecutive reaction involving the formation of bright sites which subsequently react to form dark sites. The origin of these sites and the possibility of more complex reaction mechanisms involving long-lived metastable species remain in debate. Here, we extend the Dujardin model to account for the difference in selectivity observed between the faulted and unfaulted subunits of the 7 × 7 unit cell. We measure the site-specific evolution of surface stress associated with oxidation of the Si(111)-7 × 7 surface. We demonstrate that the observed relaxation in tensile surface stress is greatest for faulted subunits of the 7 × 7 unit cell, consistent with the known larger tensile stress of these subunits. In addition, the evolution of surface stress is pressure independent, suggesting the absence of time-dependent metastable species with significant stress signatures. The implications for the room-temperature reaction mechanism are discussed.

Experiments were performed in an ultrahigh vacuum chamber containing a scanning tunneling microscope (Omicron STM-1) modified for *in situ* surface stress measurements using thin cantilever samples [12]. Figure 1(a) shows a schematic of the surface stress measurement system. One end of the sample [60 × 5 × 0.3 mm^3, *n*-type phosphorous-doped Si(111) single side polished wafers with resistivity 0.008–0.012 Ω cm] was clamped (*A*) and stress-induced deflection was calculated by the change in capacitance measured between the free end of the sample and one of the electrodes (*B* and *B′*) using an Andeen-Hagerling AH2550A capacitance bridge. The second electrode acts as a reference. Sample cleaning and surface preparation were performed locally via electron bombardment to create a 7 × 7 region (*D*) approximately 7 × 5 mm^2 in size, on an otherwise oxidized surface. The quality of the 7 × 7 reconstruction was confirmed using STM [Fig. 1(b)]. The chamber base pressure was 5×10^{-11} Torr and measured using a cold cathode (Televac 7FC) to eliminate sample heating effects.

The Si(111)-7 × 7 surface is a multilayer reconstruction [13,14] consisting of a diamond-shaped unit cell containing 19 dangling bonds. The top layer consists of 12 ad-

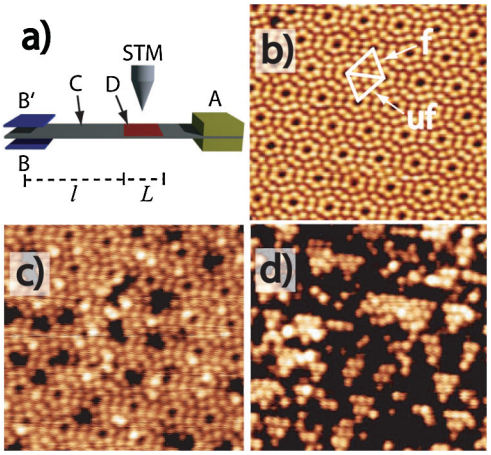

FIG. 1 (color). (a) Schematic of the surface stress measurement system (see text). (b)–(d) Unoccupied state images of Si(111)-7 × 7 before and after oxygen exposures (1.3 V and 0.06 nA). (b) Clean Si(111)-7 × 7; the unit cell is highlighted in white, with faulted (f) and unfaulted (uf) subunits; (c) 0.4 L exposure; (d) 7 L exposure.

atoms with dangling bonds arranged into two triangular subunits [Fig. 1(b)]. The underlying rest layer contains 6 additional dangling bonds. The unit cell contains unfaulted (uf) and faulted (f) subunits, which give rise to local differences in electronic structure and surface stress [15–17].

We investigated the reaction of molecular oxygen with the Si(111)-7 × 7 surface for a range of oxygen exposures and coverages. Figures 1(c) and 1(d) show unoccupied state STM images following exposures of 0.4 and 7 L of oxygen gas (1 L = 10^{-6} Torr sec), respectively. The 7 × 7 periodicity is retained even at exposures above 50 L (see supplementary information [18]). We note that, in agreement with Dujardin *et al.* [11], both bright and dark reacted adatom sites are clearly observed in Fig. 1(c) and that the latter dominate at high coverages. The rest-atom sites are not considered to react under room-temperature oxidation conditions, although this is still a matter of some dispute [5,7,19,20]. Figure 2 shows the results of a statistical analysis of the STM images (approximately 500 unit cells) acquired following oxygen exposures up to 53 L, together with possible adatom reaction geometries. Note it is possible to combine each of the oxygen inserted products (*ins* species) with adatom dangling bond products [*ad* (for "adsorbing"), *paul* (for Pauling, end-on model), and *grif* (for Griffith) structures] to describe, for example, an *ad-ins* product. Each insertion product is expected to make a large compressive surface stress contribution, whereas the adatom dangling bond products make a smaller tensile contribution.

Figure 2(a) shows the experimentally determined coverage of bright (red dots) and dark (black squares) sites as a function of oxygen exposure. While the number of dark sites is found to increase with increasing exposure, the number of bright sites increases at first and subsequently decreases thereafter. This behavior is in good agreement with the model proposed by Dujardin *et al.* [11], which describes the reaction in terms of an unreacted adatom state A reacting to form a bright intermediate state B with rate constant k_1, followed by subsequent reaction to a dark, fully reacted state D with rate constant k_2 ($A \rightarrow^{k_1} B \rightarrow^{k_2} D$). Describing k_1 and k_2 in terms of oxygen exposure (d) and assuming the rate constants are time and pressure independent, the coverage of bright sites, Θ_B, and dark sites, Θ_D, can be described by

$$\Theta_B(d) = (e^{(-k_1 d)} - e^{(-k_2 d)})k_1/(k_2 - k_1), \quad (1)$$

$$\Theta_D(d) = 1 - (k_2 e^{(-k_1 d)} - k_1 e^{(-k_2 d)})/(k_2 - k_1). \quad (2)$$

The structure of these reacted sites remains uncertain. Dujardin *et al.* attribute bright sites to molecular oxygen adsorbed at an adatom site (*paul* or *grif*) [11]. Some authors attribute bright sites to having one or more oxygen atoms inserted into adatom backbonds ($n \times ins$) [1,4,9,10], while others suggest an oxygen molecule bridging a rest atom and an adatom [7]. Dark sites have been attributed to two or more oxygen atoms inserted into the backbonds of an adatom capped by an oxygen molecule ($n \times ins\text{-}paul$) or a single oxygen atom ($n \times ins\text{-}ad$) [4,9,10]. Long-lived metastable structures have also been proposed [1,3,4,7] and will be discussed later.

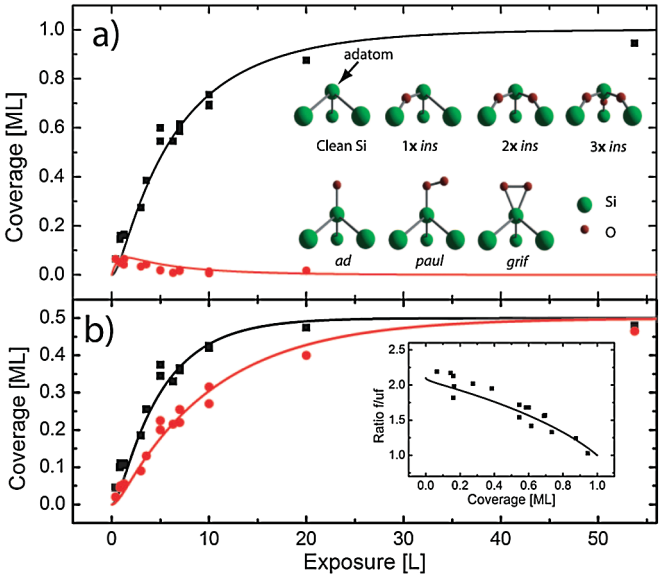

FIG. 2 (color). (a) Coverage of bright sites (red dots) and dark sites (black squares) determined by STM as function of oxygen exposure. A monolayer of bright (dark) sites has been defined as all adatoms appearing bright (dark). Solid lines represent the bright and dark site coverages predicted by the model described herein. Inset: Structures representing components of possible reaction products. (b) Dark site coverage of faulted (black squares) and unfaulted (red dots) halves of the unit cell. Solid lines represent the dark site coverage predicted by the model described in this Letter. Inset: Ratio of faulted to unfaulted dark site coverage.

The Dujardin model, however, does not account for the preference for reaction with faulted subunits [see Fig. 1(d)]. Figure 2(b) shows the results of a more detailed statistical analysis that accounts for this preference. For clarity, the small population of bright sites is omitted. The experimentally determined dark site coverage is presented in terms of faulted (black squares) and unfaulted (red dots) subunit coverages as a function of oxygen exposure. The dark site coverage was calculated using Eq. (2) but with different rate constant values for the faulted (k_{1f} = 0.21 L^{-1}, k_{2f} = 1.7 L^{-1}) and unfaulted (k_{1uf} = 0.1 L^{-1}, k_{2uf} = 1.7 L^{-1}) subunits, shown as the black curves and red curves, respectively. The value for k_2 was taken from the earlier work by Dujardin *et al.* [11], and the ratio of k_{1f}/k_{1uf} was determined experimentally from the ratio of the initial coverages at faulted and unfaulted subunits [see inset Fig. 2(b)]. These values are in good agreement with theoretical calculations, which predict that k_2 should be greater than k_1 [21] and the model provides a good fit of the experimental data in Fig. 2.

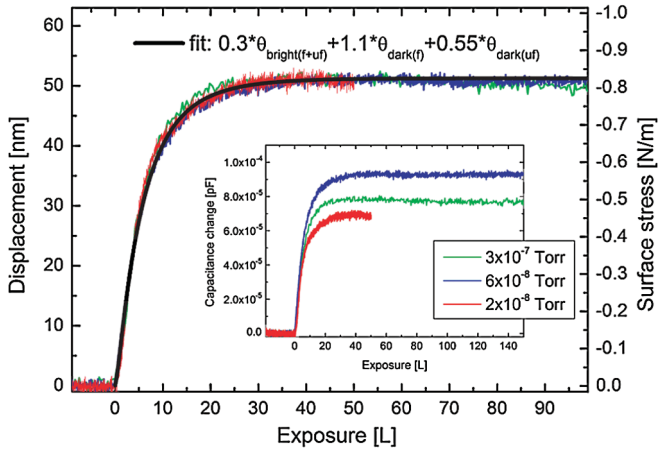

FIG. 3 (color). Capacitively measured change in surface stress (red, green, and blue lines) as function of oxygen exposure. Solid black line represents the calculated change in surface stress (see text). The graphs have been rescaled using the data shown in the inset. Inset: Capacitance changes as function of oxygen exposure. The red curve was obtained with near-equal pressures at the polished and unpolished surfaces of the sample, while for blue curves and green curves the pressure at the polished surface was higher [factor of 60 (± 6)] by use of a dosing tube.

We now consider the stress evolution during oxidation. The change in reaction-induced surface stress was monitored using the stress measurement technique shown in Fig. 1(a). Figure 3 (inset) shows the change in capacitance as a function of oxygen exposure recorded with (blue lines and green lines) and without (red line) a dosing tube directed at the sample. The displacement (Δd) of the sample was calculated from the observed change in capacitance. The change in surface stress ($\Delta\sigma$) was determined using the Stoney equation [22], $\Delta\sigma = Et^2/6R(1-\nu)$, where $E/(1-\nu)$ is the elastic constant for Si(111) (2.29×10^{11} N m^{-2} [23]), t is the sample thickness (300 ± 20 μm), and $1/R$ is the curvature of the sample, which was calculated using [12] $1/R = \Delta d/(L^2/2 + Ll)$, where L is the length of the reaction area (7 ± 1 mm), and l is the distance from the reaction area to the center of the capacitance electrode (27 ± 1 mm) [see Fig. 1(a)]. Saturation coverage of the surface results in a compressive change in surface stress of -0.82 ± 0.25 N m^{-1} [0.66 eV/(1×1) unit cell].

We note that the shape of each curve in Fig. 3 (inset) is solely a function of the actual surface coverage and is not dependent on exposure time or pressure. The different saturation levels displayed in the inset of Fig. 3 are due to variations in the prepared 7×7 surface area and the size of the stress accumulating terraces. Despite these variations the stress evolution can be arbitrarily rescaled to produce the single curve shown in Fig. 3. Two conclusions can be drawn. First, the stress contribution from the unpolished back side of the sample is negligible compared to that of the polished side. This is supported by the fact that a consistent curve shape is observed regardless of whether a dosing tube is used or not, and that there is only a modest reduction in the saturation value associated with the red curve, where no dosing tube was used. Second, changes in surface stress depend only on oxygen coverage, i.e., the stress evolution is not dependent of the combination of exposure time and pressure, over large time scales and pressures. For instance, saturation was achieved in $\approx$100 sec at $P_{O2} = 3 \times 10^{-7}$ Torr and $\approx$1500 sec at $P_{O2} = 2 \times 10^{-8}$ Torr. An immediate consequence is that any metastable species that might exist on this surface during room-temperature oxidation cannot have a significant stress fingerprint (see below).

The observed stress evolution can be related to the site-specific oxygen coverage using the kinetic model by assuming different stress contributions from bright and dark reaction sites observed within the faulted and unfaulted subunits. The resulting calculated change in surface stress was fitted to the experimental data assuming that surface stress is additive, i.e., that the stress induced by two reactive sites is twice that of a single site. The best fit to the stress data is the solid line in Fig. 3 which is given by $\Delta\sigma = (0.3\Theta_{B(\mathrm{f+uf})}) + (1.1\Theta_{D(\mathrm{f})}) + (0.55\Theta_{D(\mathrm{uf})})$.

These estimated stress signatures warrant comment. Dark sites appear to contribute more to the overall change in surface stress than bright sites. This would be consistent with a greater number of oxygen atoms inserted into the adatom backbonds in dark sites relative to bright sites. However, since the number of bright sites is small and peaks at small exposures (Fig. 2), their net contribution to the overall change in surface stress is very small, the fit in Eq. (2) is least sensitive to bright sites, although the values shown provide the best overall fit to the stress evolution over the time course of the reaction.

Second, dark sites within faulted subunits contribute more to the net change in surface stress than those in unfaulted subunits. This behavior can be understood by recognizing that the entire 7×7 surface has an intrinsic tensile surface stress [16,17]. This is mainly caused by the adatom bonding configuration that pulls inwards on each of the three rest-layer atoms to which it is bonded [16,17]. Vanderbilt and Meade estimated this contribution to be $\approx +1.7$ eV/(1×1) unit cell. The presence of a stacking fault contributes an additional tensile stress component (+0.23–0.4 eV/(1×1) unit cell [16,17] to the faulted subunits. These findings were confirmed by Brommer *et al.* in a complete calculation of the 7×7 unit cell [24]. It is therefore reasonable that the insertion of an oxygen atom into a Si-Si backbond will result in the partial release of the intrinsic stress of the 7×7 reconstruction. This is consistent with calculations that indicate an average intrinsic surface stress of $+1.9$ eV/(1×1) unit cell on the clean 7×7, while the observed relaxation following oxygen saturation is -0.66 eV/(1×1) unit cell (Fig. 3). The relaxation is larger in faulted subunits due to the presence

TABLE I. Literature reaction mechanisms.

Model	Bright	Intermediate state	Dark
A [9,10]	$2 \times ins$	$\cdots$	$ad\text{-}3 \times ins$
B [4]	$2 \times ins$	$paul\text{-}2 \times ins$	$ad\text{-}2 \times ins$
C [4]	ins	$paul\text{-}ins$	$ad\text{-}2 \times ins$

of a larger intrinsic stress in these regions. These findings are also consistent with the preservation of the underlying intrinsically tensile 7×7 reconstruction following saturation (see [18]). We note, however, that these data differ from those of Sander and Ibach [25] who estimated a compressive change in surface stress of -7.2 N/m [5.8 eV/(1×1) unit cell], which would lead to a final compressive stress of ≈ -3.9 eV/(1×1) unit cell.

We now discuss these findings in the context of three possible reaction mechanisms in which the intermediate decays spontaneously into dark sites (Table I). Mechanism *A* is fully consistent with our experimental observations. There is no intermediate product and dark sites have more inserted atoms than bright sites, and hence a larger stress, consistent with our data. Mechanism *B* could be consistent but only if we allow bright and dark sites to make similar stress contributions (due to similar numbers of inserted atoms in *B*). Mechanism *C*, on the other hand, is not consistent with our experimental observations, since the time-dependent insertion of an additional oxygen into the adatom backbond is expected to have a significant time-dependent stress signature, which is not consistent with the data in Fig. 3.

In conclusion, the oxidation of Si(111)-7×7 can be described as a two-step reaction with different reactivities for the faulted and unfaulted subunits. We described the quantitative relationship between site-specific oxygen coverage and the observed increase in compressive surface stress. We estimate the stress signatures for different reaction products and show that there are no long-lived intermediates at room temperature that exhibit a significant stress fingerprint. At this juncture it is not possible to determine the actual structures associated with the bright and dark sites. However, with the aid of calculations and the present stress study, it may be possible to eliminate some species identified in Fig. 2. Finally, the combination of STM and surface stress presented here holds considerable promise in the elucidation of a wide range of surface chemical phenomena.

The financial support of Science Foundation Ireland (Grant No. 06/IN.1/I106) is gratefully acknowledged. The authors thank Maxi Mrusek for her help with the statistical analysis.

*Present address: Institute for Molecular Science, 38 Nishigo-Naka, Myodaiji, Okazaki 444-8585, Japan.
†Present address: Institute of Physics, Martin-Luther-Universität Halle-Wittenberg, 06120 Halle (Saale), Germany.
‡Corresponding author.
jboland@tcd.ie

[1] S. H. Lee and M. H. Kang, Phys. Rev. Lett. **82**, 968 (1999).
[2] S. H. Lee and M. H. Kang, Phys. Rev. B **61**, 8250 (2000).
[3] F. Matsui, H. W. Yeom, K. Amemiya, K. Tono, and T. Ohta, Phys. Rev. Lett. **85**, 630 (2000).
[4] K. Sakamoto, H. M. Zhang, and R. I. G. Uhrberg, Phys. Rev. B **68**, 075302 (2003).
[5] K. Sakamoto, H. M. Zhang, and R. I. G. Uhrberg, Phys. Rev. B **70**, 035301 (2004).
[6] M. H. Tsai, Y. H. Tang, I. S. Hwang, and T. T. Tsong, Phys. Rev. B **66**, 241304 (2002).
[7] T. Hoshino and Y. Nishioka, Phys. Rev. B **61**, 4705 (2000).
[8] H. Okuyama, T. Aruga, and M. Nishijima, Phys. Rev. Lett. **91**, 256102 (2003).
[9] H. Okuyama, Y. Ohtsuka, and T. Aruga, J. Chem. Phys. **122**, 234709 (2005).
[10] A. J. Mayne, F. Rose, G. Comtet, L. Hellner, and G. Dujardin, Surf. Sci. **528**, 132 (2003).
[11] G. Dujardin, A. Mayne, G. Comtet, L. Hellner, M. Jamet, E. LeGoff, and P. Millet, Phys. Rev. Lett. **76**, 3782 (1996).
[12] T. Narushima, N. T. Kinahan, and J. J. Boland, Rev. Sci. Instrum. **78**, 053903 (2007).
[13] K. Takayanagi, Y. Tanishiro, M. Takahashi, and S. Takahashi, J. Vac. Sci. Technol. A **3**, 1502 (1985).
[14] K. Takayanagi, Y. Tanishiro, S. Takahashi, and M. Takahashi, Surf. Sci. **164**, 367 (1985).
[15] J. A. Kubby and J. J. Boland, Surf. Sci. Rep. **26**, 61 (1996).
[16] D. Vanderbilt, Phys. Rev. Lett. **59**, 1456 (1987).
[17] R. D. Meade and D. Vanderbilt, Phys. Rev. B **40**, 3905 (1989).
[18] See supplementary material at http://link.aps.org/supplemental/10.1103/PhysRevLett.104.146101 showing that surfaces retain the 7×7 periodicity at high exposures.
[19] K. Sakamoto, S. T. Jemander, G. V. Hansson, and R. I. G. Uhrberg, Phys. Rev. B **65**, 155305 (2002).
[20] I. S. Hwang, R. L. Lo, and T. T. Tsong, Phys. Rev. Lett. **78**, 4797 (1997).
[21] P. Sonnet, L. Stauffer, and C. Minot, Surf. Rev. Lett. **6**, 1031 (1999).
[22] G. G. Stoney, Proc. R. Soc. A **82**, 172 (1909).
[23] W. A. Brantley, J. Appl. Phys. **44**, 534 (1973).
[24] K. D. Brommer, M. Needels, B. E. Larson, and J. D. Joannopoulos, Phys. Rev. Lett. **68**, 1355 (1992).
[25] D. Sander and H. Ibach, Phys. Rev. B **43**, 4263 (1991).